

1 **Multi-isotope labelling of organic matter by diffusion**
2 **of $^2\text{H}/^{18}\text{O}$ -vapour and ^{13}C - CO_2 into the leaves and its**
3 **distribution within the plant**

4 **M. S. Studer^{1,2}, R. T. W. Siegwolf², M. Leuenberger³, S. Abiven¹**

5 [1] Department of Geography, University of Zurich, Winterthurerstr. 190, 8057
6 Zurich, Switzerland

7 [2] Laboratory of Atmospheric Chemistry, Paul Scherrer Institute, 5232 Villigen PSI,
8 Switzerland

9 [3] Climate and Environmental Physics, Physics Institute and Oeschger Centre for
10 Climate Change Research, University of Bern, Sidlerstr. 5, 3012 Bern

11 Correspondence to: Dr. S. Abiven (samuel.abiven@geo.uzh.ch)

12 **Abstract**

13 Isotope labelling is a powerful tool to study elemental cycling within terrestrial
14 ecosystems. Here we describe a new multi-isotope technique to label organic matter
15 (OM).

16 We exposed poplars (*Populus deltoides x nigra*) for 14 days to an atmosphere
17 enriched in $^{13}\text{CO}_2$ and depleted in $^2\text{H}_2^{18}\text{O}$. After one week, the water-soluble leaf OM
18 ($\delta^{13}\text{C} = 1346 \pm 162 \text{ ‰}$) and the leaf water were strongly labelled ($\delta^{18}\text{O} = -63 \pm 8 \text{ ‰}$,
19 $\delta^2\text{H} = -156 \pm 15 \text{ ‰}$). The leaf water isotopic composition was between the
20 atmospheric and stem water, indicating a considerable back-diffusion of vapour into
21 the leaves (58 - 69 %) in opposite direction to the net transpiration flow that itself is
22 reflected by the stem water resembling soil water composition. The atomic ratios of
23 the labels recovered ($^{18}\text{O}/^{13}\text{C}$, $^2\text{H}/^{13}\text{C}$) were 2 - 4 times higher in leaves than in the
24 stems and roots. This either indicates the synthesis of more condensed compounds
25 (lignin vs. cellulose) in roots and stems, or be the result of O and H exchange and
26 fractionation processes during transport and biosynthesis.

27 We demonstrate that the three major OM elements (C, O, H) can be labelled and
28 traced simultaneously within the plant. This approach could be of interdisciplinary
29 interest for the fields of plant physiology, paleoclimatic reconstruction or soil science.

30

31 **1 Introduction**

32 Artificial labelling with stable isotopes facilitates the observation of bio(geo)chemical
33 cycling of elements or compounds with minor disturbance to the plant-soil systems. It
34 has provided many insights into plant carbon allocation patterns (e.g. Simard et al.
35 1997; Keel et al. 2006; Högberg et al. 2008), water dynamics (e.g. in Plamboeck et al.
36 2007; Kulmatiski et al. 2010) and soil organic matter processes (e.g. in Bird and Torn
37 2006; Girardin et al. 2009) in terrestrial ecosystems. Only a few studies used labelling
38 approaches with more than one stable isotope, for example to study the interactions
39 between the carbon and nitrogen cycle (e.g. in Bird and Torn 2006; Schenck zu
40 Schweinsberg-Mickan et al. 2010). However, to our knowledge isotopic labelling of
41 organic matter (OM) with its three major elements, carbon (C), oxygen (O) and
42 hydrogen (H), has never been done in ecosystem studies before, even though
43 combined $\delta^{13}\text{C}$, $\delta^{18}\text{O}$ and $\delta^2\text{H}$ analyses have been widely used to study plant
44 physiological processes and to reconstruct past climatic conditions (Hangartner et al.,
45 2012; Roden and Farquhar, 2012; Scheidegger et al., 2000; Werner et al., 2012).
46 Similarly, an artificial labelling with those isotopes would be useful to clarify basic
47 mechanisms related to the plant water-use efficiency or the oxygen and hydrogen
48 signals in tree rings, but also to study other OM dynamics in the plant-soil system
49 such as OM decomposition in the soil.

50 The C, O and H contents of organic matter have been applied to distinguish major
51 groups of compounds, by plotting the atomic ratios O/C and H/C in a van Krevelen
52 diagram (Kim et al., 2003; Ohno et al., 2010; Sleighter and Hatcher, 2007). This
53 approach is based on the distinct molecular composition of organic compounds. For
54 example the glucose molecule ($\text{C}_6\text{H}_{12}\text{O}_6$) is characterized by high O/C (= 1) and H/C
55 (= 2) ratios and is the precursor of other compounds, such as cellulose ($(\text{C}_6\text{H}_{10}\text{O}_5)_{[n]}$)
56 O/C = 0.8, H/C = 1.7, Fig. 3a). Condensation or reduction reactions during
57 biosynthesis lead to other compound groups with lower atomic ratios (e.g. lignin) or
58 similar H/C, but lower O/C ratios (e.g. lipids, proteins) compared to glucose.
59 Following the logic of the van Krevelen diagram, we wanted to test, if we can use the
60 isotopic ratios $^{18}\text{O}/^{13}\text{C}$ and $^2\text{H}/^{13}\text{C}$ of the labels recovered in plant-soil bulk materials
61 after labelling the fresh assimilates with those stable isotopes, to detect the utilization
62 of the labelled assimilates for the synthesis of different OM compounds. With this
63 multi-labelling approach we would gain information about the characteristics of the

64 OM formed by simple isotopic analysis of bulk material. This has several advantages
65 compared to compound specific analysis, such as being much less laborious and less
66 expensive and yield integrated information on the bulk organic matter sampled.

67 In this study we added the ^{13}C , ^{18}O and ^2H labels via the gaseous phase in the plants'
68 atmosphere (CO_2 , water vapour). Pre-grown plants were exposed to the labelled
69 atmosphere continuously for fourteen days under laboratory conditions and the labels
70 added were traced in different plant compartments (leaves, petioles, new stems, stem
71 cuttings, roots) and soil organic matter at different points in time. We applied a simple
72 isotope mixing model to estimate the fraction of ^{18}O and ^2H that entered the leaf by
73 diffusion from the atmosphere into the leaf intercellular cavities and plotted the
74 atomic and isotopic ratios of the OM formed in van Krevelen diagrams to test if the
75 multi-isotope labelling approach can be used to detect changes in the OM
76 characteristics.

77 **2 Material and Methods**

78 **2.1 Plants and soil**

79 The soil (cambisol) was sampled from the upper 15 cm in a beech forest ($8^\circ 33' \text{ E}$, 47°
80 $23' \text{ N}$, 500 m elevation), coarse sieved (2.5 x 3.5 cm) and large pieces of hardly
81 decomposed organic material were removed. The soil had a clay loam texture, a pH of
82 4.8, an organic C content of 2.8 % and a C/N ratio of 11. The plant pots (volume = 8.2
83 dm^3) were filled with 3018 ± 177 g soil (dry weight equivalent). 15 Poplar seedlings
84 (*Populus deltoides x nigra*, Dorskamp clone) were grown indoors from 20 cm long
85 stem cuttings for five weeks before they were transferred into labelling chambers
86 (described below). They were kept in the chamber for acclimatization for one week
87 prior to labelling. At the beginning of the labelling experiments, the average dry
88 weight of fresh plant biomass (without the original stem cutting) was 3.3 ± 0.1 g and
89 the average total leaf area was 641 ± 6 cm^2 per plant. At the end of the experiment
90 (last sampling) the dry weight was 5.4 ± 1.1 g and the total leaf area was 1354 ± 161
91 cm^2 . The leaf area was measured with a handheld area meter (CID-203 Laser leaf area
92 meter, CID Inc.).

93 **2.2 Labelling chamber, procedure and environmental conditions**

94 The labelling chambers (MICE - Multi-Isotope labelling in a Controlled Environment
95 - facility) provide a hermetical separation of the shoots (leaves, petioles and new

96 stems) from the roots, rhizosphere and the soil. The plant shoots are enclosed by one
97 large polycarbonate cuboid (volume 1.2 m³) with a removable front plate and five 2
98 cm wide gaps in the bottom plate to slide in three plants in each row. Small
99 polycarbonate pieces, Kapton tape and a malleable sealant (Terostat IX, Henkel AG &
100 Co.) wrapped around the stem cuttings were used to seal off the upper from the lower
101 chamber. The belowground compartments (soil and roots) are in fifteen individual
102 pots, which are hermetically sealed from the laboratory and aerated with outdoor air.
103 This setup ensures that all plants receive the same labelling treatment and prevents the
104 diffusion of labelled atmospheric gases into the soil.

105 The environmental conditions in the MICE facility are automatically controlled and
106 monitored by a software (programmed with LabVIEW, National Instruments
107 Switzerland Corp.) switching on/off the light sources (Xenon, HELLA KGaA Hueck &
108 Co) and valves to in- or exclude instruments to regulate the CO₂ and H₂O
109 concentration, which is measured by an infrared gas analyzer (LI-840, LI-COR Inc.).
110 The chamber air is fed by a vacuum pump (N 815, KNF Neuberger AG) through
111 perforated glass tubes within a water reservoir to humidify the air or through a Peltier
112 cooled water condenser to dry the air (Appendix Fig. A1). Further the chamber air can
113 be fed through a Plexiglas tube filled with Soda lime to absorb the CO₂ or CO₂ is
114 injected from a gas cylinder.

115 The isotope labels (¹³C, ¹⁸O and ²H) were added continuously for 14 days via gaseous
116 phase to the plant shoots. We used CO₂ enriched in ¹³C (10 atom% ¹³C-CO₂,
117 Cambridge Isotope Laboratories, Inc.), and water vapour depleted in ¹⁸O and ²H ($\delta^{18}\text{O}$
118 = - 370 ‰ and $\delta^2\text{H}$ = - 813 ‰, waste product from enrichment columns at the Paul
119 Scherrer Institute). Thus the labelled gases added were enriched by 8.90 atom% ¹³C
120 and depleted by 0.07 atom% ¹⁸O and 0.01 atom% ²H relative to the ambient air.

121 The soil moisture was maintained at 100 % field capacity and the relative air humidity
122 was 74 %, in order to promote the back-diffusion of water into the leaves. The light
123 intensity was low ($80 \pm 25 \mu\text{mol m}^{-2} \text{s}^{-1}$ photosynthetic active radiation), and the CO₂
124 concentration was kept at 508 ± 22 ppm in order to maintain a high atmospheric
125 carbon supply. The day-night cycles were twelve hours and the temperature within the
126 labelling chamber was 31 ± 3 °C throughout the experiments.

127 **2.3 Sample collection**

128 The plant-soil systems were destructively harvested at five sampling dates (three
129 replicates each) to detect the dynamics of the labelling over time,. The first sampling
130 was done one day before the labelling experiment started (unlabelled control, referred
131 to as $t = 0$). Subsequently plant-soil systems were sampled after 1, 2, 8 and 14 days of
132 continuous labelling.

133 At each sampling date the plant-soil systems were separated into leaves, petioles,
134 stems, cuttings, roots (washed with deionised water and carefully dabbed with tissue)
135 and bulk soil (visible roots were removed with tweezers). The leaves (sub-sample of
136 six leaves) were sampled all along the stem (homogeneously distributed). The
137 uppermost leaves, newly formed during the experiment (completely labelled), were
138 excluded, since we wanted to study the tracer uptake and translocation dynamics in
139 already existing leaves prior to the treatment. In one out of the three plant replicates
140 we took two leaf sub-samples from distinct positions along the shoot. We sampled six
141 leaves from the upper and six leaves from the lower half of the shoot (thereafter
142 referred to as "top" and "bottom", respectively). Leaves, stems, roots and bulk soil
143 were collected in airtight glass vials and frozen immediately at $- 20\text{ }^{\circ}\text{C}$ for later
144 cryogenic vacuum extraction of the tissue water. Cuttings and petioles were dried for
145 24 hours at $60\text{ }^{\circ}\text{C}$.

146 The tissue water was extracted with cryogenic vacuum extraction by heating the
147 frozen samples within the sampling vials in a water bath at $80\text{ }^{\circ}\text{C}$ under a vacuum
148 (10^{-3} mbar) for two hours. The evaporating water was collected in U-vials submersed
149 in a liquid nitrogen cold trap. After thawing (within the closed U-vials), the water
150 samples were transferred into vials and stored frozen at $- 20\text{ }^{\circ}\text{C}$ for later $\delta^{18}\text{O}$ and $\delta^2\text{H}$
151 analysis. To study the water dynamics, additional water vapour samples from the
152 chamber air were collected by peltier-cooled water condensers (in an external air
153 circuit connected to the plant labelling chamber) and analysed for $\delta^{18}\text{O}$ and $\delta^2\text{H}$.

154 The dried plant residues of the cryogenic vacuum extraction were used for isotopic
155 bulk analyses (described below). The leaf water-soluble organic matter was extracted
156 by hot water extraction. 60 mg milled leaf material was dissolved in 1.5 ml of
157 deionised water and heated in a water bath ($85\text{ }^{\circ}\text{C}$) for 30 min. After cooling and
158 centrifugation ($10'000\text{ g}$, 2 min), the supernatant was freeze-dried and analysed for

159 $\delta^{13}\text{C}$. $\delta^2\text{H}$ analyses were not possible on the hot water extracts (mainly sugars), due to
160 incomplete equilibration with ambient water vapour (Filot, 2010).

161 **2.4 Isotopic and elemental analyses**

162 All samples were milled to a fine powder with a steel ball mill and weighed into tin
163 ($\delta^{13}\text{C}$ analyses) or silver ($\delta^{18}\text{O}$ and $\delta^2\text{H}$ analyses) capsules and measured by isotope-
164 ratio mass spectrometry (IRMS). The $\delta^{13}\text{C}$ samples were combusted at 1700 °C in an
165 elemental analyser (EA 1110, Carlo Erba) and the resulting CO_2 was transferred in a
166 helium stream via a variable open-split interface (ConFlo II, Finnigan MAT) to the
167 IRMS (Delta S, Thermo Finnigan; see Werner et al. 1999). The samples for $\delta^{18}\text{O}$
168 analyses were pyrolysed at 1040 °C in an elemental analyser (EA 1108, Carlo Erba)
169 and transferred via ConFlo III interface (Thermo Finnigan) to the IRMS (Delta plus
170 XL, Thermo Finnigan). The samples for $\delta^2\text{H}$ analyses were equilibrated with water
171 vapour of known signature prior to the IRMS measurements, to determine the isotopic
172 signature of the non-exchangeable hydrogen (as described in Filot et al. 2006;
173 Hangartner et al. 2012). After equilibration the samples were pyrolysed in a
174 thermochemical elemental analyser (TC/EA, Thermo-Finnigan) at a temperature of
175 1425 °C and the gaseous products were carried by a helium stream via a ConFlow II
176 open split interface (Thermo Finnigan) into the IRMS (Isoprime, Cheadle). The
177 amount of exchangeable hydrogen (25-27%) and oxygen (2-3%) was measured for
178 the leaf, stem and root tissue using depleted water vapour to equilibrate the samples.
179 The measurement precisions of the solid sample analyses were 0.12 ‰ $\delta^{13}\text{C}$, 0.54 ‰
180 $\delta^{18}\text{O}$ and 1 ‰ $\delta^2\text{H}$ and were assessed by working standards measured frequently
181 along with the experimental samples. The precisions were lower than reported for
182 measurements of natural abundance, since highly labelled sample material was
183 analysed.

184 Elemental C, H and N content of solid samples was analysed in an elemental analyzer
185 (CHN-900, Leco Corp.) and the elemental O content by RO-478 (Leco Corp.).

186 The liquid samples from the cryogenic vacuum extraction (tissue water) were
187 pyrolysed in an elemental analyser (TC/EA, Thermo Finnigan) and the evolving CO
188 and H_2 gases were transferred via the ConFlo III interface (Thermo Finnigan) to a
189 IRMS (Delta plus XL, Thermo Finnigan) for oxygen and hydrogen isotope ratio
190 analysis (Gehre et al., 2004). The precision of the liquid sample measurement was \pm
191 0.75 ‰ $\delta^{18}\text{O}$ and \pm 1.59 ‰ $\delta^2\text{H}$.

192 **2.5 Calculations**

193 Isotopic ratios were expressed in delta (δ) notation as the deviation (in ‰) from the
 194 international standards Vienna Pee Dee Belemnite (V-PDB, $^{13}\text{C}/^{12}\text{C} = 1.11802 \times 10^{-2}$)
 195 and Vienna Standard Mean Ocean Water (V-SMOW, $^{18}\text{O}/^{16}\text{O} = 2.0052 \times 10^{-3}$ and
 196 $^2\text{H}/^1\text{H} = 1.5575 \times 10^{-4}$). The significance of changes in isotopic signature between the
 197 sampling dates and the unlabelled control ($t = 0$) were statistically tested by t-tests
 198 performed by R software (R Core Team 2014).

199 In the following paragraphs we describe first the calculations for the leaf water source
 200 partitioning (Eqs. 1 - 4). These equations are given for the oxygen isotope (^{18}O), but
 201 they apply also for hydrogen (^2H). Then we describe the calculations for the relative
 202 recovery of the isotopes ($^{18}\text{O}/^{13}\text{C}$ and $^2\text{H}/^{13}\text{C}$) in the bulk organic matter (Eqs. 5 - 7).

203 The leaf water isotopic signature (at steady state) can be described by a model of
 204 Dongmann et al. (1974) to calculate leaf water H_2^{18}O enrichment, a derivative of
 205 Craig & Gordon (1965) (Eq. 1). According to this model, the isotopic signature of the
 206 leaf water (L) is the result of kinetic (ϵ^k) and equilibrium (ϵ^*) fractionation processes
 207 during evaporation of the source water (S) within the leaves and the back-diffusion of
 208 atmospheric water vapour (V) into the leaves as affected by relative air humidity (h).

209
$$\delta^{18}\text{O}_L = \delta^{18}\text{O}_S + \epsilon^k + \epsilon^* + (\delta^{18}\text{O}_V - \delta^{18}\text{O}_S - \epsilon^k) \cdot h \quad (1)$$

210 We used a two-source isotope mixing model (Eq. 2, principles described in Dawson et
 211 al. 2002) to assess the contribution of the two main water pools (soil and atmospheric
 212 water) to the leaf water based on its isotopic signatures. An overview on the input data
 213 for the mixing model is given as in Appendix A (Fig. A1).

214
$$f_{source,2} = \frac{\delta^{18}\text{O}_{leaf,water} - \delta^{18}\text{O}_{source,1}}{\delta^{18}\text{O}_{source,2} - \delta^{18}\text{O}_{source,1}} \quad (2)$$

215 , where $\delta^{18}\text{O}_{leaf,water}$ is the isotopic signature (in ‰) of water extracted from the leaves
 216 at a specific sampling date and $\delta^{18}\text{O}_{source,1}$ and $\delta^{18}\text{O}_{source,2}$ are the theoretical isotopic
 217 signatures of the leaf water if all water would originate either from the soil (source 1)
 218 or the atmospheric (source 2) water pool.

219 The first source, thereafter referred to as "evaporating source", represents the water
 220 taken up from the soil by the roots, which is transported via the xylem to the leaf,
 221 where it evaporates. The isotopic signature of the evaporating source (Eq. 3) is

222 estimated by the maximum leaf water enrichment that would occur at 0 % relative air
 223 humidity i.e. by the first part of the Dongmann approach (solving Eq. 1 with $h = 0$).

$$224 \quad \delta^{18}\text{O}_{source,1} = \delta^{18}\text{O}_{stem,water} + \epsilon^k + \epsilon_{atm}^* \quad (3)$$

225 , where $\delta^{18}\text{O}_{stem,water}$ is the isotopic signature (in ‰) of the water extracted from the
 226 stem tissue (approximating the xylem water) and ϵ^k and ϵ_{atm}^* are the kinetic and
 227 equilibrium fractionation terms, respectively, at the specific sampling date.

228 The second source, thereafter called "condensation source", refers to the water vapour
 229 that diffuses from the atmosphere into the leaves and condensates at the cell walls.
 230 The contribution of this source would be maximal at 100 % relative humidity, which
 231 results in Eq. 4 when solving Eq. 1 with $h = 1$.

$$232 \quad \delta^{18}\text{O}_{source,2} = \delta^{18}\text{O}_{atm,vap} + \epsilon_{atm}^* = \delta^{18}\text{O}_{atm,cond} - \epsilon_{pelt}^* + \epsilon_{atm}^* \quad (4)$$

233 , where $\delta^{18}\text{O}_{atm,vap}$ is the isotopic signature of the water vapour of the chamber
 234 atmosphere and ϵ_{atm}^* is the equilibrium fractionation inside the chamber at the specific
 235 sampling date. The signature of the atmospheric water vapour was measured on its
 236 condensate ($\delta^{18}\text{O}_{atm,cond}$) collected in the peltier water trap, which was therefore
 237 corrected with the equilibrium fractionation during condensation inside the peltier-
 238 cooled water condenser (ϵ_{pelt}^*).

239 The kinetic fractionation due to the difference in molecular diffusivity of the water
 240 molecule species ($\epsilon^k = 20.7$ ‰ $\delta^{18}\text{O}$ and 10.8 ‰ $\delta^2\text{H}$) was estimated according to
 241 Cappa et al. (2003) for a laminar boundary layer (Schmidt-number $q = 2/3$,
 242 Dongmann et al. 1974). The equilibrium fractionation due to the phase change during
 243 evaporation and condensation at different temperatures was calculated as in Majoube
 244 (1971) with the conditions present at the specific day. The condensation (dew point)
 245 temperature inside the peltier-cooled water condenser ($T_{pelt,DP}$) was determined based
 246 on the remaining humidity and the air pressure of the air leaving the condenser
 247 (details on the calculation are given in Appendix B). The equilibrium fractionation
 248 factors during the labelling experiment were on average $\epsilon_{atm}^* = 8.9 \pm 0.2$ ‰ for $\delta^{18}\text{O}$
 249 and 72.7 ± 2.7 ‰ for $\delta^2\text{H}$ at $T = 31.3 \pm 2.7$ °C inside the labelling chamber and $\epsilon_{pelt}^* =$
 250 11.1 ± 0.2 ‰ for $\delta^{18}\text{O}$ and 103.3 ± 3.3 ‰ for $\delta^2\text{H}$ at $T_{pelt,DP} = 6.0 \pm 2.5$ °C inside the
 251 water condenser.

252 We compared the distribution of the assimilated labels (^{13}C , ^{18}O , ^2H) in the leaf, stem
 253 and root tissue by its isotopic ratios. Therefore we converted the δ -notation to atom
 254 fraction (Eq. 5) according to Coplen (2011).

$$255 \quad x(^{13}\text{C})_{t=x} = \frac{1}{1 + \frac{1}{(\delta^{13}\text{C}_{t=x}/1000 + 1) \cdot R_{V-PDB}}} \quad (5)$$

256 , where $\delta^{13}\text{C}_{t=x}$ is the isotopic signature (in ‰) of the bulk tissue at sampling date x
 257 and R is the ratio of the heavier to the lighter isotope ($^{13}\text{C}/^{12}\text{C}$) of the international
 258 standard V-PDB. The atom fraction of ^{18}O and ^2H was calculated accordingly, but
 259 using R_{V-SMOW} as reference and neglecting the ^{17}O isotope amount.

260 For the van Krevelen approach we calculated the elemental ratios. The relative
 261 label distribution ($^{18}\text{O}/^{13}\text{C}$ and $^2\text{H}/^{13}\text{C}$) within the plant organic matter (OM) was
 262 calculated based on the excess atom fraction measured in each tissue (Eq. 6).

$$263 \quad \frac{x^E(^{18}\text{O}_{tissue,OM})_{t=x/t=0}}{x^E(^{13}\text{C}_{tissue,OM})_{t=x/t=0}} = \frac{x(^{18}\text{O}_{tissue,OM})_{t=x} - x(^{18}\text{O}_{tissue,OM})_{t=0}}{x(^{13}\text{C}_{tissue,OM})_{t=x} - x(^{13}\text{C}_{tissue,OM})_{t=0}} \quad (6)$$

264 , where $x^E(^{18}\text{O})_{t=x/t=0}$ and $x^E(^{13}\text{C})_{t=x/t=0}$ is the excess atom fraction of the labels detected
 265 at a specific sampling date ($t = x$), relative to the unlabelled control ($t = 0$). Eq. 6 and
 266 7 was analogously calculated for the $^2\text{H}/^{13}\text{C}$ ratio.

267 In a second step we corrected the isotopic ratios ($^{18}\text{O}/^{13}\text{C}$ and $^2\text{H}/^{13}\text{C}$) with the
 268 maximum label strength of the precursor of the plant organic matter, i.e. the
 269 maximum label strength of fresh assimilates (Eq. 7). The maximum ^{13}C label strength
 270 was approximated by the ^{13}C excess atom fraction relative to the unlabelled control
 271 (x^E) measured in the leaf water-soluble organic matter (wsOM) and the maximum ^{18}O
 272 and ^2H label strength by the excess atom fraction measured in the leaf water. The leaf
 273 water is the direct source of hydrogen in assimilates and the indirect source of oxygen
 274 via the atmospheric CO_2 dissolved in water (Schmidt et al., 2001, 2003). The oxygen
 275 isotope composition of dissolved CO_2 equilibrates immediately with the leaf water
 276 signature, whereby carbonic anhydrase catalyzes this process and induces a
 277 temperature dependent kinetic ^{18}O fractionation (Gillon and Yakir, 2000; Uchikawa
 278 and Zeebe, 2012). The fractionation was assumed to be constant in this experiment
 279 with controlled temperature and was thus omitted by the calculation of the excess
 280 atom fraction.

$$281 \quad \frac{x_{norm}^E \left({}^{18}\text{O}_{tissue, OM} \right)_{t=x / t=0}}{x_{norm}^E \left({}^{13}\text{C}_{tissue, OM} \right)_{t=x / t=0}} = \frac{x^E \left({}^{18}\text{O}_{tissue, OM} \right)_{t=x / t=0}}{x^E \left({}^{13}\text{C}_{tissue, OM} \right)_{t=x / t=0}} \cdot \frac{x^E \left({}^{13}\text{C}_{leaf, wsOM} \right)_{t=x / t=0}}{x^E \left({}^{18}\text{O}_{leaf, water} \right)_{t=x / t=0}} \quad (7)$$

282 **3 Results**

283 **3.1 Labelling of the leaf water and water-soluble OM**

284 The ^{18}O and ^2H label added as water vapour to the chamber atmosphere ($\delta^{18}\text{O} = - 370$
 285 ‰ , $\delta^2\text{H} = - 813 \text{‰}$), was mixed with transpired water, which was isotopically
 286 enriched compared to the added label (Fig. 1). The isotopic signature of the water
 287 vapour within the chamber air stabilized after four days at a level of $- 112 \pm 4 \text{‰}$ $\delta^{18}\text{O}$
 288 and $- 355 \pm 7 \text{‰}$ $\delta^2\text{H}$. Thus the atmospheric water vapour signature was depleted in
 289 ^{18}O by $94 \pm 4 \text{‰}$ and in ^2H by $183 \pm 7 \text{‰}$ compared to the unlabelled atmosphere.

290 The leaf water was strongly depleted and its isotopic signature was stable at a level of
 291 $- 64 \pm 7 \text{‰}$ for $\delta^{18}\text{O}$ and $- 158 \pm 13 \text{‰}$ for $\delta^2\text{H}$ already after two days of labelling with
 292 the depleted water vapour (Fig. 1). The leaf water was thus on average depleted by 63
 293 $\pm 7 \text{‰}$ for $\delta^{18}\text{O}$ and $126 \pm 14 \text{‰}$ for $\delta^2\text{H}$ compared to the unlabelled leaf water
 294 signature and it was between the signature of the atmospheric water vapour and the
 295 water added to the soil ($\delta^{18}\text{O} = - 9 \pm 0 \text{‰}$, $\delta^2\text{H} = - 74 \pm 2 \text{‰}$). This indicates that a
 296 substantial amount of the leaf water originated from the atmospheric water pool,
 297 suggesting that it entered the leaf via diffusion through the stomata. The depletion of
 298 the water within a leaf was dependent on its position on the shoot (Fig. 2c,e). The leaf
 299 water of the leaves sampled in the upper half of the shoot was $7 \pm 2 \text{‰}$ and $18 \pm 8 \text{‰}$
 300 less depleted in $\delta^{18}\text{O}$ and $\delta^2\text{H}$ than the leaves sampled at the lower half. The isotopic
 301 signature of the stem water ($\delta^{18}\text{O} = - 10 \pm 0 \text{‰}$ and $\delta^2\text{H} = - 74 \pm 4 \text{‰}$), as well as the
 302 root ($\delta^{18}\text{O} = - 6 \pm 1 \text{‰}$ and $\delta^2\text{H} = - 58 \pm 4 \text{‰}$) and the soil water ($\delta^{18}\text{O} = - 6 \pm 1 \text{‰}$
 303 and $\delta^2\text{H} = - 63 \pm 3 \text{‰}$), was not significantly depleted and reflected the signature of
 304 the water added to the soil (Fig. 1).

305 At the second sampling date, the leaf water seemed to be more depleted than the water
 306 vapour within the chamber air (Fig. 1). This is the result of different sampling
 307 procedures. The leaf sampling was performed at one point in time (three hours after
 308 the light switched on), while the atmospheric water vapour collected by condensation
 309 represents an average on the previous 24 hours. Therefore the depletion of the water
 310 vapour is underestimated before the equilibrium of the isotopic signature in the
 311 atmosphere was reached. In the following the average values of signatures detected

312 after the equilibrium was reached are given ($t = 8$ and $t = 14$). We tried to estimate the
313 contribution of the isotopic signature of the atmospheric water vapour that enters the
314 leaf by diffusion with a two-source mixing model (Tab. 1). The results were obtained
315 by the two water isotopes ^{18}O and ^2H separately. Both indicated a substantial
316 contribution of the atmospheric water vapour to the leaf water isotopic signature,
317 whereby the estimates based on the oxygen isotope yielded a higher contribution (69
318 ± 7 %) than the hydrogen estimates (58 ± 4 %). The estimates for the leaves sampled
319 at different position on the shoot varied by 5 %, whereas the contribution of
320 atmospheric water to the leaf water was higher in the leaves sampled at the bottom
321 (71 ± 4 % based on ^{18}O and 60 ± 2 % based on ^2H) than in the leaves at the top ($66 \pm$
322 2 % and 55 ± 0 %, respectively) of the shoots.

323 The ^{13}C - CO_2 added (8938 ‰ $\delta^{13}\text{C}$) was assumingly also strongly diluted by respired
324 ^{12}C - CO_2 , but we did not measure the isotopic signature of the CO_2 within the chamber
325 air. The leaf water-soluble OM was significantly enriched already after one day of
326 labelling and levelled off towards the end of the experiment. At the last two sampling
327 dates its isotopic signature was on average 1346 ± 162 ‰ $\delta^{13}\text{C}$.

328 **3.2 Labelling of the bulk organic matter**

329 All three applied labels could be detected in the plant bulk material (Tab. 2). We
330 measured the isotopic signature of the non-exchangeable hydrogen, which was
331 estimated to be 74 ± 1 % of the total OM. After fourteen days of continuous labelling,
332 the leaves, petioles, stems and roots were enriched by 650 - 1150 ‰ in $\delta^{13}\text{C}$, depleted
333 by 4 - 17 ‰ in $\delta^{18}\text{O}$ and 6 - 31 ‰ in $\delta^2\text{H}$. Thus the plant biomass was significantly
334 labelled even under the extreme environmental conditions (high temperature and low
335 light availability) that were critical for net C assimilation (increasing tissue respiration
336 and reducing photosynthesis, respectively). However, the labelling was not strong
337 enough to trace the OM within the large OM pools of the cuttings and soil organic
338 matter, in which the change in isotopic signature was close to the detection limit or
339 could not be detected. The measured depletion in ^{18}O of the bulk soil can be
340 accounted for natural variability, since the same effect has been observed in non-
341 treated soil (data not shown here).

342 The labelling of the leaf bulk OM occurred in parallel to the labelling of the leaf water
343 and water-soluble OM (Fig. 2). The leaf OM was enriched in ^{13}C after one day (Fig.
344 2b) and depleted in ^{18}O and ^2H after two days (Fig. 2d,f). The incorporation of the

345 label into the leaf OM was, as the labelling of the leaf water, dependent on the
346 position on the shoot. The biomass of the leaves at the top was more enriched in ^{13}C
347 (by up to 673 ‰) than the biomass of the leaves at the bottom of the shoots, and in
348 contrast to the leaf water, more depleted in ^{18}O and ^2H (by up to 9 and 21 ‰,
349 respectively) at the top than at the bottom. This indicates a higher overall assimilation
350 in the leaves at the top of the shoot.

351 **3.3 Atomic and isotopic ratios to characterize organic matter**

352 The atomic ratios of the plant bulk OM were in the range of 13.7 - 115.4 C/N, 0.70 -
353 0.83 O/C and 1.56 - 1.72 H/C (Tab. 3). The leaf OM was characterized by the lowest
354 C/N and O/C ratios and concurrently by highest H/C ratios (Fig. 3a). The other plant
355 tissues indicated a linear trend in decreasing O/C and H/C and increasing C/N ratios
356 in the order of stems, petioles, roots and cuttings.

357 The recovery of the three isotopes varied between the leaf, stem and root tissue, while
358 they were similar between the sampling dates (Fig. 3b). The isotopic ratios of the
359 excess atom fractions were $3.5 \pm 0.4 \times 10^{-3} \text{ }^{18}\text{O}/^{13}\text{C}$ and $5.3 \pm 0.5 \times 10^{-4} \text{ }^2\text{H}/^{13}\text{C}$ in the
360 leaves, $1.4 \pm 0.1 \times 10^{-3} \text{ }^{18}\text{O}/^{13}\text{C}$ and $2.9 \pm 0.6 \times 10^{-4} \text{ }^2\text{H}/^{13}\text{C}$ in the stems and $1.0 \pm 0.2 \times$
361 $10^{-3} \text{ }^{18}\text{O}/^{13}\text{C}$ and $1.0 \pm 1.4 \times 10^{-4} \text{ }^2\text{H}/^{13}\text{C}$ in the roots after the equilibrium in the leaf
362 water and water-soluble OM labelling was reached. Thus the $^{18}\text{O}/^{13}\text{C}$ ratios were on
363 average 2.6 (± 0.2) times lower in the stems and 3.8 (± 0.7) times lower in the roots
364 than in the leaves (Tab. 3) and the $^2\text{H}/^{13}\text{C}$ ratios 1.9 (± 0.2) and 3.1 (± 0.6) times lower
365 in the stems and roots, respectively, than in the leaves.

366 After correction for the maximum label strength (^{18}O , ^2H and ^{13}C excess atom fraction
367 within the leaf water and the water-soluble OM, respectively), the isotopic ratios were
368 in the range of 0.17 - 0.43 $^{18}\text{O}/^{13}\text{C}$ and 0.14 - 0.23 $^2\text{H}/^{13}\text{C}$. The normalized isotopic
369 ratios were thus in the magnitude order of the atomic ratios reported for OM
370 compounds (Tab. 3, Fig. 3c), however lower than expected for fresh organic matter
371 (in the range characteristic for condensed hydrocarbons).

372 **4 Discussion**

373 **4.1 Diffusion of atmospheric water vapour into the leaf**

374 The strong depletion in $\delta^{18}\text{O}$ and $\delta^2\text{H}$ observed in the leaf water indicates a high back-
375 diffusion of labelled water vapour from the atmosphere into the leaf. The diffusion is
376 dependent on the gradient between atmospheric and leaf water vapour pressure and

377 the stomatal conductance (Parkhurst, 1994). The higher the atmospheric water vapour
378 pressure (the smaller the gradient), the more water molecules diffuse back into the
379 leaf. The latter is further enhanced the larger the stomatal conductance is (Reynolds
380 Henne, 2007). Here we maintained the atmospheric vapour pressure constant at a high
381 level, ensuring a high back-diffusion at a given stomatal conductance. In our
382 experiment the leaf water $\delta^{18}\text{O}$ and $\delta^2\text{H}$ signature is determined by i) the signature and
383 the amount of labelled (depleted) water vapour diffusing into the leaf intercellular
384 cavities, ii) by the enrichment due to transpiration (kinetic and equilibrium
385 fractionation) and iii) by the influx of xylem water, which is isotopically enriched
386 relative to the labelled water vapour. The latter is proportionally enhanced by
387 increasing transpiration rates as a result of the diffusion convection process of H_2O
388 (Péclet effect, Farquhar and Lloyd 1993).

389 The distinct label signal in the water sampled in leaves at different positions on the
390 shoot indicates differences in the transpiration rate. Meinzer et al. (1997)
391 demonstrated in large poplar trees that shading or lower irradiance leads to lower
392 stomatal conductance and transpiration rates. Thus the back-diffusion in the leaves on
393 the bottom might have been reduced due to lower stomatal conductance. However, the
394 increased transpiration in the leaves at the top, lead to an even stronger dilution of the
395 isotopic signal in the leaf water due to i) increased evaporative leaf water enrichment
396 and ii) the Péclet effect (enhanced influx of xylem water, which was enriched
397 compared to the labelled atmospheric water vapour).

398 The amount of leaf water that entered the leaf by back-diffusion was estimated to be
399 58-69 %. This result is in contradiction to the common perception that most of the leaf
400 water is taken up from the soil via roots. However it is in line with the observations
401 made by Farquhar & Cernusak (2005), who modelled the leaf water isotopic
402 composition in the non-steady state and estimated the contribution of atmospheric
403 water to the leaf water to be approximately two-thirds of the total water supply.
404 Albeit, our estimates are based on a modelling approach that does not take into
405 account the Péclet effect or daily fluctuations in the isotopic signatures as described
406 below, our estimates correspond very well the findings of Farquhar & Cernusak
407 (2005).

408 The model used to estimate the quantitative contribution of the two water sources is
409 based on the measured signature of the leaf water ($\delta^{18}\text{O}_{\text{leaf,water}}$) and the estimated

410 signatures of the water at the evaporating and condensation site ($\delta^{18}\text{O}_{\text{source},1}$ and
411 $\delta^{18}\text{O}_{\text{source},2}$, respectively). The “dilution” of the (laminar) leaf water with the relatively
412 enriched xylem water through the Péclet effect is included in the $\delta^{18}\text{O}_{\text{leaf,water}}$. This
413 explains the lower contribution of atmospheric water (- 5 %) estimated in the leaves
414 sampled at the top (due to the Péclet effect resulting from higher transpiration rates)
415 compared to the leaves sampled at the bottom of the shoot.

416 Some inaccuracy in the two-source mixing model estimates might have been
417 introduced by daily fluctuations in the environmental and labelling conditions. The
418 mixture ($\delta^{18}\text{O}_{\text{leaf,water}}$) was sampled after three hours of light, whereas the estimation
419 of the two sources ($\delta^{18}\text{O}_{\text{source},1}$ and $\delta^{18}\text{O}_{\text{source},2}$) is based on daily average values of
420 environmental parameters and the atmospheric water vapour ($\delta^{18}\text{O}_{\text{atm,vap}}$) label
421 strength. In our experiment, fluctuations in $\delta^{18}\text{O}_{\text{atm,vap}}$ were caused by adding the
422 labelled vapour mainly during night-time, when transpiration was low. Thus the
423 atmospheric label strength was assumingly highest before the lights were switched on
424 and gradually diluted during the day by transpired water vapour. Hence the actual
425 $\delta^{18}\text{O}_{\text{atm,vap}}$ at the time of plant sampling was probably more depleted than the
426 measured average signature. Therefore $\delta^{18}\text{O}_{\text{source},2}$ and its contribution to the leaf
427 water was slightly overestimated. The effect of the temperature fluctuations ($\pm 3\text{ }^{\circ}\text{C}$)
428 via changes in the equilibrium fractionation was minor for the outcome of the mixing
429 model $< 1\%$.

430 Nonetheless, the strong depletion of the leaf water in ^2H and ^{18}O proofs, that back-
431 diffusion of atmospheric water vapour into the leaf is an important mechanisms for
432 leaf water uptake. This supports the hypothesis that atmospheric water vapour
433 diffusion might be as important as the flux of water from the xylem into the leaf (at
434 least under humid conditions) and be an important mechanisms for the reversed water
435 flow observed in the tropics (Goldsmith, 2013). Furthermore, these results
436 demonstrate that the leaf water isotopic composition is strongly affected by the
437 atmospheric signature at humid conditions and that thus the applicability of the dual-
438 isotope approach (Scheidegger et al., 2000), e.g. to reconstruct past climate conditions
439 by tree ring analysis, is only valid if the source water and atmospheric vapour $\delta^{18}\text{O}$
440 are similar. The back-diffusion of atmospheric vapour at high humidity could be
441 another factor next to the evaporative enrichment (as demonstrated by Roden and

442 Farquhar, 2012) to overshadow the effects of stomatal conductance on the leaf $\delta^{18}\text{O}$
443 signature.

444 **4.2 Tracing organic matter?**

445 The O/C and H/C ratio of the plant bulk material was close to the signature of
446 cellulose (Fig. 3a). The leaves had a lower O/C ratio with a constant high H/C ratio
447 indicating that its OM contains more reduced compounds such as amino-sugars or
448 proteins, which is also supported by its low C/N ratio. The trend of decreasing O/C
449 and H/C ratios observed in the other tissues is in the direction of condensation
450 reactions. This trend most likely indicates the increasing lignification of OM from
451 shoots, to roots, to cuttings.

452 The same trend has been observed in the ratios of the labels added from the leaf, to
453 the stem, to the root OM (Fig. 3b,c). The lower isotopic O/C and H/C ratios in the
454 root and stem tissue compared to the leaf tissue could indicate the utilization of the
455 labelled assimilates for the synthesis of more condensed compounds (e.g. lignin) in
456 those tissues. However, other factors affecting the isotopic ratios of the OM are the
457 maximum label strength, the exchange of hydrogen and oxygen with xylem water
458 during transport and biosynthesis and the isotopic fractionation during metabolism.

459 The isotopic ratios (Fig. 3b) were around three magnitudes smaller than the expected
460 atomic ratios of OM (Sleighter and Hatcher, 2007). This is mainly due to the different
461 maximum label strength, which was highest for the ^{13}C and lowest for the ^2H . After
462 correction for this factor, the isotopic ratios were in the range of the atomic ratios
463 characteristic for condensed hydrocarbons (Fig. 3c). The isotopic ratios might be
464 lower than expected due to inaccurate approximation of the maximum label strength
465 of fresh assimilates (by the leaf water and water-soluble OM), or be the result of ^{18}O
466 and ^2H label losses during transport and biosynthesis.

467 One reason for the label loss might be the use of other (more enriched) sources during
468 biosynthesis. For example O_2 (enriched by 23 ‰ $\delta^{18}\text{O}$) has been identified as a further
469 source for aromatic compounds, such as phenols and sterols (Schmidt et al., 2001).
470 However, for hydrogen, water is the only known source (Schmidt et al., 2003) and
471 therefore the use of other O or H sources during biosynthesis can not explain the
472 (major) loss of the ^{18}O and ^2H label.

473 Another potential reason would be the kinetic fractionation during biosynthesis that
474 leads to distinct isotopic signatures of different OM compounds (described in Schmidt

475 et al. 2001, 2003; Badeck et al. 2005; Bowling et al. 2008). However, assuming
476 constant isotopic fractionation during the experimental period (constant
477 environmental conditions), the isotopic ratios would not be affected, since they are
478 based on the excess atom fraction relative to the unlabelled OM.

479 A third reason for the loss of the ^{18}O and ^2H label could be the exchange of hydrogen
480 and oxygen atoms with water. O and H exchanges with tissue water during transport
481 and the synthesis of new compounds (as recently discussed for oxygen in phloem
482 sugars and cellulose in Offermann et al. 2011 and Gessler et al. 2013). O of carbonyl
483 groups (Barbour, 2007; Sternberg et al., 1986) and H in nucleophilic OH and NH
484 groups or H adjacent to carbonyl groups (Augusti et al., 2006; Garcia-Martin et al.,
485 2001) exchange with water. Thus biochemical reactions lead to different isotopomers
486 of organic compounds (Augusti and Schleucher, 2007). The proportion of O and H
487 exchanged can be considerable, e.g. during cellulose synthesis around 40 % of O and
488 H are exchanged with the tissue water (Roden and Ehleringer, 1999; Yakir and
489 DeNiro, 1990). The exchange with water explains to some extent the stronger relative
490 ^{18}O and ^2H signal in the leaf OM compared to the stem and root OM, since the leaf
491 water was labelled, while the stem and root water was not. Especially the $^{18}\text{O}/^{13}\text{C}$
492 isotopic ratios were increased in the leaf OM compared to the relations observed in
493 the atomic ratios (Fig. 3a). The leaf OM has the lowest O/C atomic ratios while it has
494 the highest $^{18}\text{O}/^{13}\text{C}$ isotopic ratios of all plant compartments (Tab. 3). This effect is
495 less expressed for the $^2\text{H}/^{13}\text{C}$ ratios, since only the fraction of hydrogen that does not
496 exchange with ambient water vapour is measured. The non-exchangeable fraction (74
497 %) is hydrogen bound to carbon (Filot et al., 2006), which is hardly exchanged with
498 xylem water.

499 **5 Conclusions**

500 We present a new technique to label organic matter at its place of formation by the
501 application of labels through the gaseous phase ($^{13}\text{CO}_2$ and $^2\text{H}_2^{18}\text{O}$). In this study we
502 could show that in a humid atmosphere, the atmospheric water vapour isotopic
503 signature dominates the leaf water signature, due to a strong back-diffusion of water
504 vapour into the leaf. Further we detected differences in the relative distribution of ^{13}C ,
505 ^{18}O and ^2H in the leaves, stems and roots. This could indicate the synthesis of
506 different compounds in the particular tissues (change in OM characteristics), but it
507 could also be the result of exchange and fractionation processes during transport and

508 biosynthesis. To further test these two possibilities a better estimation of the
509 maximum label strength by compound specific sugar analysis would be needed,
510 which has been further developed for $\delta^{13}\text{C}$ (Rinne et al., 2012) and for $\delta^{18}\text{O}$ (Zech et
511 al., 2013) recently, but does not yet exist for $\delta^2\text{H}$ analysis.

512 The multi-isotope labelling technique can be used to assess the amount of vapour
513 diffusing into the leaves and to trace the dynamics of the labelled organic matter. It
514 could be applied in soil sciences, e.g. to track the decomposition pathways of soil OM
515 inputs, or in the field of plant physiology and paleoclimatic reconstruction, e.g. to
516 further investigate the O and H exchange and fractionation processes during transport
517 and metabolic processes or the importance of the ambient air humidity besides its
518 isotopic composition for the climate signal stored in tree-ring cellulose. Furthermore
519 the multi-isotope labelling technique has the potential to make changes of OM
520 characteristics visible (e.g. C allocation into the non-structural vs. structural pool), for
521 example after a change in climatic conditions, and to trace the labelled OM during its
522 decomposition within the soil.

523 **Acknowledgements**

524 This study was funded by the Swiss National Science Foundation (SNSF), project
525 number 135233. We would like to thank Professor M. W. I Schmidt for his support,
526 M. Saurer for his comments on the manuscript, R. Künzli, I. Lötscher, R. Maier, P.
527 Nyfeler and I. Woodhatch for technical assistance, and the soil science and
528 biogeochemistry (University of Zurich) and the ecosystem fluxes (Paul Scherrer
529 Institute) research groups for valuable discussions.

530 **References**

- 531 Augusti, A., Betson, T. R. and Schleucher, J.: Hydrogen exchange during cellulose
532 synthesis distinguishes climatic and biochemical isotope fractionations in tree rings,
533 *New Phytol.*, 172, 490–499, doi:10.1111/j.1469-8137.2006.01843.x, 2006.
- 534 Augusti, A. and Schleucher, J.: The ins and outs of stable isotopes in plants, *New*
535 *Phytol.*, 174, 473–475, doi:10.1111/j.1469-8137.2007.02075.x, 2007.
- 536 Badeck, F.-W., Tcherkez, G., Nogués, S., Piel, C. and Ghashghaie, J.: Post-
537 photosynthetic fractionation of stable carbon isotopes between plant organs - a
538 widespread phenomenon, *Rapid Commun. Mass Spectrom.*, 19, 1381–1391,
539 doi:10.1002/rcm.1912, 2005.

540 Barbour, M. M.: Stable oxygen isotope composition of plant tissue: a review, *Funct.*
541 *Plant Biol.*, 34, 83–94, doi:10.1071/FP06228, 2007.

542 Bird, J. A. and Torn, M. S.: Fine roots vs. needles: a comparison of ^{13}C and ^{15}N
543 dynamics in a ponderosa pine forest soil, *Biogeochemistry*, 79, 361–382,
544 doi:10.1007/s10533-005-5632-y, 2006.

545 Bowling, D. R., Pataki, D. E. and Randerson, J. T.: Carbon isotopes in terrestrial
546 ecosystem pools and CO_2 fluxes, *New Phytol.*, 178, 24–40, doi:10.1111/j.1469-
547 8137.2007.02342.x, 2008.

548 Cappa, C. D., Hendricks, M. B., Depaolo, D. J. and Cohen, R. C.: Isotopic
549 fractionation of water during evaporation, *J. Geophys. Res.*, 108, 4525,
550 doi:10.1029/2003JD003597, 2003.

551 Coplen, T. B.: Guidelines and recommended terms for expression of stable-isotope-
552 ratio and gas-ratio measurement results, *Rapid Commun. Mass Spectrom.*, 25,
553 2538–2560, doi:10.1002/rcm.5129, 2011.

554 Craig, H. and Gordon, L. I.: Deuterium and oxygen 18 variations in the ocean and the
555 marine atmosphere, in *Stable isotopes in oceanographic studies and*
556 *paleotemperatures*, edited by E. Tongiorgi, pp. 9–130, Spoleto, Pisa, Italy., 1965.

557 Dawson, T. E., Mambelli, S., Plamboeck, A. H., Templer, P. H. and Tu, K. P.: Stable
558 isotopes in plant ecology, *Annu. Rev. Ecol. Syst.*, 33, 507–559,
559 doi:10.1146/annurev.ecolsys.33.020602.095451, 2002.

560 Dongmann, G., Nürnberg, H. W., Förstel, H. and Wagener, K.: On the enrichment of
561 H_2^{18}O in the leaves of transpiring plants, *Radiat. Environ. Biophys.*, 11, 41–52,
562 doi:10.1007/BF01323099, 1974.

563 Farquhar, G. D. and Cernusak, L. A.: On the isotopic composition of leaf water in the
564 non-steady state, *Funct. Plant Biol.*, 32, 293–303, doi:10.1071/FP04232, 2005.

565 Farquhar, G. D. and Lloyd, J.: Carbon and oxygen isotope effects in the exchange of
566 CO_2 between terrestrial plants and the atmosphere, in *Stable isotopes and plant*
567 *carbon-water relations*, edited by J. R. Ehleringer, A. E. Hall, and G. D. Farquhar,
568 pp. 47–70, Academic Press, Waltham., 1993.

569 Filot, M.: *Isotopes in tree-rings: Development and application of a rapid preparative*
570 *online equilibration method for the determination of D / H ratios of*
571 *nonexchangeable hydrogen in tree-ring cellulose*, 106 pp., Bern., 2010.

572 Filot, M. S., Leuenberger, M., Pazdur, A. and Boettger, T.: Rapid online equilibration
573 method to determine the D/H ratios of non-exchangeable hydrogen in cellulose,
574 *Rapid Commun. Mass Spectrom.*, 20, 3337–3344, doi:10.1002/rcm, 2006.

575 Garcia-Martin, M. L., Ballesteros, P. and Cerda, S.: The metabolism of water in cells
576 and tissues as detected by NMR methods, *Prog. Nucl. Magn. Reson. Spectrosc.*, 39,
577 41–77, doi:10.1016/S0079-6565(01)00031-0, 2001.

578 Gehre, M., Geilmann, H., Richter, J., Werner, R. A. and Brand, W. A.: Continuous
579 flow $^2\text{H}/^1\text{H}$ and $^{18}\text{O}/^{16}\text{O}$ analysis of water samples with dual inlet precision, *Rapid*
580 *Commun. Mass Spectrom.*, 18, 2650–2660, doi:10.1002/rcm.1672, 2004.

581 Gessler, A., Brandes, E., Keitel, C., Boda, S., Kayler, Z. E., Granier, A., Barbour, M.,
582 Farquhar, G. D. and Treydte, K.: The oxygen isotope enrichment of leaf-exported
583 assimilates - does it always reflect lamina leaf water enrichment?, *New Phytol.*, 200,
584 144–157, doi:10.1111/nph.12359, 2013.

585 Gillon, J. S. and Yakir, D.: Internal conductance to CO_2 diffusion and C^{18}O
586 discrimination in C_3 Leaves, *Plant Physiol.*, 123, 201–213, doi:10.1104/pp.123.1.
587 201, 2000.

588 Girardin, C., Rasse, D. P., Biron, P., Ghashghaie, J. and Chenu, C.: A method for ^{13}C -
589 labeling of metabolic carbohydrates within French bean leaves (*Phaseolus vulgaris*
590 L.) for decomposition studies in soils, *Rapid Commun. Mass Spectrom.*, 23, 1792–
591 1800, doi:10.1002/rcm, 2009.

592 Goldsmith, G. R.: Changing directions : the atmosphere-plant–soil continuum, *New*
593 *Phytol.*, 199, 4–6, 2013.

594 Hangartner, S., Kress, A., Saurer, M., Frank, D. and Leuenberger, M.: Methods to
595 merge overlapping tree-ring isotope series to generate multi-centennial
596 chronologies, *Chem. Geol.*, 294, 127–134, doi:10.1016/j.chemgeo.2011.11.032,
597 2012.

598 Högberg, P., Högberg, M. N., Göttlicher, S. G., Betson, N. R., Keel, S. G., Metcalfe,
599 D. B., Campbell, C., Schindlbacher, A., Hurry, V., Lundmark, T., Linder, S. and
600 Näsholm, T.: High temporal resolution tracing of photosynthate carbon from the tree
601 canopy to forest soil microorganisms, *New Phytol.*, 177, 220–228,
602 doi:10.1111/j.1469-8137.2007.02238.x, 2008.

603 Keel, S. G., Siegwolf, R. T. W. and Körner, C.: Canopy CO_2 enrichment permits
604 tracing the fate of recently assimilated carbon in a mature deciduous forest, *New*
605 *Phytol.*, 172, 319–329, doi:10.1111/j.1469-8137.2006.01831.x, 2006.

606 Kim, S., Kramer, R. W. and Hatcher, P. G.: Graphical method for analysis of
607 ultrahigh-resolution broadband mass spectra of natural organic matter, the van
608 Krevelen diagram, *Anal. Chem.*, 75, 5336–5344, doi:10.1021/ac034415p, 2003.

609 Kulmatiski, A., Beard, K. H., Verweij, R. J. T. and February, E. C.: A depth-
610 controlled tracer technique measures vertical, horizontal and temporal patterns of
611 water use by trees and grasses in a subtropical savanna, *New Phytol.*, 188, 199–209,
612 doi:10.1111/j.1469-8137.2010.03338.x, 2010.

613 Majoube, M.: Fractionnement en oxygène 18 et en deutérium entre l'eau et sa vapeur,
614 *J. Chim. Phys. physico-chimie Biol.*, 68, 1423–1435, 1971.

615 Meinzer, F. C., Hinckley, T. M. and Ceulemans, R.: Apparent responses of stomata to
616 transpiration and humidity in a hybrid poplar canopy, *Plant, Cell Environ.*, 20,
617 1301–1308, doi:10.1046/j.1365-3040.1997.d01-18.x, 1997.

618 Offermann, C., Ferrio, J. P., Holst, J., Grote, R., Siegwolf, R. T. W., Kayler, Z. E. and
619 Gessler, A.: The long way down-are carbon and oxygen isotope signals in the tree
620 ring uncoupled from canopy physiological processes?, *Tree Physiol.*, 31, 1088–
621 1102, doi:10.1093/treephys/tpr093, 2011.

622 Ohno, T., He, Z., Sleighter, R. L., Honeycutt, C. W. and Hatcher, P. G.: Ultrahigh
623 resolution mass spectrometry and indicator species analysis to identify marker
624 components of soil- and plant biomass- derived organic matter fractions, *Environ.*
625 *Sci. Technol.*, 44, 8594–8600, doi:10.1021/es101089t, 2010.

626 Parkhurst, D. F.: Tansley review no. 65. Diffusion of CO₂ and other gases inside
627 leaves, *New Phytol.*, 126, 449–479, doi:10.1111/j.1469-8137.1994.tb04244.x, 1994.

628 Plamboeck, A. H., Dawson, T. E., Egerton-Warburton, L. M., North, M., Bruns, T. D.
629 and Querejeta, J. I.: Water transfer via ectomycorrhizal fungal hyphae to conifer
630 seedlings, *Mycorrhiza*, 17, 439–447, doi:10.1007/s00572-007-0119-4, 2007.

631 Reynolds Henne, C. E.: A study of leaf water $\delta^{18}\text{O}$ composition using isotopically-
632 depleted H₂¹⁸O-vapour, in *Climate-isotope relationships in trees under non-limiting*
633 *climatic conditions from seasonal to century scales*, pp. 77–92, University of Bern.,
634 2007.

635 Rinne, K. T., Saurer, M., Streit, K. and Siegwolf, R. T. W.: Evaluation of a liquid
636 chromatography method for compound-specific $\delta^{13}\text{C}$ analysis of plant carbohydrates
637 in alkaline media, *Rapid Commun. Mass Spectrom.*, 26, 2173–85,
638 doi:10.1002/rcm.6334, 2012.

639 Roden, J. S. and Ehleringer, J. R.: Hydrogen and oxygen isotope ratios of tree-ring
640 cellulose for riparian trees grown long-term under hydroponically controlled
641 environments, *Oecologia*, 121, 467–477, doi:10.1007/s004420050953, 1999.

642 Roden, J. S. and Farquhar, G. D.: A controlled test of the dual-isotope approach for
643 the interpretation of stable carbon and oxygen isotope ratio variation in tree rings,
644 *Tree Physiol.*, 32, 1–14, doi:10.1093/treephys/tps019, 2012.

645 Scheidegger, Y., Saurer, M., Bahn, M. and Siegwolf, R. T. W.: Linking stable oxygen
646 and carbon isotopes with stomatal conductance and photosynthetic capacity: A
647 conceptual model, *Oecologia*, 125, 350–357, doi:10.1007/S004420000466, 2000.

648 Schenck zu Schweinsberg-Mickan, M., Joergensen, R. G. and Müller, T.: Fate of ¹³C-
649 and ¹⁵N-labelled rhizodeposition of *Lolium perenne* as function of the distance to the
650 root surface, *Soil Biol. Biochem.*, 42, 910–918, doi:10.1016/j.soilbio.2010.02.007,
651 2010.

652 Schmidt, H.-L., Werner, R. A. and Eisenreich, W.: Systematics of ²H patterns in
653 natural compounds and its importance for the elucidation of biosynthetic pathways,
654 *Phytochem. Rev.*, 2, 61–85, doi:10.1023/B:PHYT.0000004185.92648.ae, 2003.

655 Schmidt, H.-L., Werner, R. A. and Rossmann, A.: O-18 pattern and biosynthesis of
656 natural plant products, *Phytochemistry*, 58, 9–32, doi:10.1016/S0031-
657 9422(01)00017-6, 2001.

658 Simard, S. W., Durall, D. M. and Jones, M. D.: Carbon allocation and carbon transfer
659 between *Betula papyrifera* and *Pseudotsuga menziesii* seedlings using a ¹³C pulse-
660 labeling method, *Plant Soil*, 191, 41–55, doi:10.1023/A:1004205727882, 1997.

661 Sleighter, R. L. and Hatcher, P. G.: The application of electrospray ionization coupled
662 to ultrahigh resolution mass spectrometry for the molecular characterization of
663 natural organic matter, *J. Massspectrometry*, 42, 559–574, doi:10.1002/jms, 2007.

664 Steinmann, K., Siegwolf, R. T. W., Saurer, M. and Körner, C.: Carbon fluxes to the
665 soil in a mature temperate forest assessed by ¹³C isotope tracing, *Oecologia*, 141,
666 489–501, doi:10.1007/s00442-004-, 2004.

667 Sternberg, L. D. S. L. O., DeNiro, M. J. D. and Savidge, R. A.: Oxygen isotope
668 exchange between metabolites and water during biochemical reactions leading to
669 cellulose synthesis, *Plant Physiol.*, 82, 423–427, doi:10.1104/pp.82.2.423, 1986.

670 Studer, M. S., Siegwolf, R. T. W. and Abiven, S.: Carbon transfer, partitioning and
671 residence time in the plant-soil system: a comparison of two ¹³CO₂ labelling
672 techniques, *Biogeosciences*, 11, 1637–1648, doi:10.5194/bg-11-1637-2014, 2014.

673 Uchikawa, J. and Zeebe, R. E.: The effect of carbonic anhydrase on the kinetics and
674 equilibrium of the oxygen isotope exchange in the CO₂-H₂O system: Implications
675 for δ¹⁸O vital effects in biogenic carbonates, *Geochim. Cosmochim. Acta*, 95, 15–
676 34, doi:10.1016/j.gca.2012.07.022, 2012.

677 Werner, C., Schnyder, H., Cuntz, M., Keitel, C., Zeeman, M. J., Dawson, T. E.,
678 Badeck, F.-W., Brugnoli, E., Ghashghaie, J., Grams, T. E. E., Kayler, Z. E., Lakatos,
679 M., Lee, X., Máguas, C., Ogée, J., Rascher, K. G., Siegwolf, R. T. W., Unger, S.,
680 Welker, J., Wingate, L. and Gessler, A.: Progress and challenges in using stable
681 isotopes to trace plant carbon and water relations across scales, *Biogeosciences*, 9,
682 3083–3111, doi:10.5194/bg-9-3083-2012, 2012.

683 Yakir, D. and DeNiro, M. J. D.: Oxygen and hydrogen isotope fractionation during
684 cellulose metabolism in *Lemna gibba* L., *Plant Physiol.*, 93, 325–332,
685 doi:10.1104/pp.93.1.325, 1990.

686 Zech, M., Saurer, M., Tuthorn, M., Rinne, K., Werner, R. a, Siegwolf, R., Glaser, B.
687 and Juchelka, D.: A novel methodological approach for δ(18)O analysis of sugars
688 using gas chromatography-pyrolysis-isotope ratio mass spectrometry., *Isotopes*
689 *Environ. Health Stud.*, 49, 492–502, doi:10.1080/10256016.2013.824875, 2013.

690
691

691 **Tables**

692 **Table 1.** Diffusion of atmospheric water vapour into the leaf water. $\delta^{18}\text{O}$ and $\delta^2\text{H}$
 693 signatures of leaf water and its two sources: i) the evaporating source (Eq. 3),
 694 estimated by the stem water signature plus kinetic and equilibrium leaf water
 695 enrichment (assuming full evaporation without back-diffusion), and ii) the
 696 condensation source (Eq. 4), assessed by the atmospheric water vapour signature plus
 697 equilibrium fractionation to account for the gas-liquid phase change. The contribution
 698 of the second source (diffusion and condensation of atmospheric water vapour) to the
 699 leaf water ($f_{\text{source},2/\text{leaf},\text{water}}$) was estimated by a two-source isotope mixing model for
 700 ^{18}O and ^2H separately (Eq. 2). Presented are the average values of three plant
 701 replicates for each sampling date \pm one standard deviation

Sampling date (days)	Leaf water ⁽¹⁾		Source 1: Evaporating source ⁽²⁾		Source 2: Condensation source ⁽²⁾		$f_{\text{source},2/\text{leaf},\text{water}}$ ⁽²⁾	
	$\delta^{18}\text{O}$ (‰)	$\delta^2\text{H}$ (‰)	$\delta^{18}\text{O}$ (‰)	$\delta^2\text{H}$ (‰)	$\delta^{18}\text{O}$ (‰)	$\delta^2\text{H}$ (‰)	^{18}O (%)	^2H (%)
0	-1.0 (±0.5)	-32.0 (±1.8)	21.3 (±0.4)	10.9 (±2.6)	-8.8	-99.7	74.2 (±1.2)	38.8 (±0.3)
1	-11.7 (±1.8)	-53.0 (±5.9)	19.5 (±0.3)	10.3 (±3.2)	-27.3	-143.3	66.6 (±3.9)	41.2 (±3.2)
2	-65.6 (±6.5)	-162.3 (±8.6)	20.0 (±0.6)	14.4 (±2.1)	-47.6	-196.0	126.6 (±9.8)	84.0 (±4.1)
8	-65.2 (±2.0)	-159.9 (±3.8)	20.0 (±0.7)	5.3 (±3.9)	-98.6	-274.8	71.8 (±1.5)	59.0 (±0.8)
14	-60.4 (±10.7)	-152.3 (±21.2)	19.3 (±0.4)	9.5 (±5.1)	-101.8	-275.8	65.8 (±8.7)	56.8 (±6.8)

⁽¹⁾ directly measured

⁽²⁾ calculated

702

702 **Table 2.** Multi-isotope labelling of bulk organic matter. $\delta^{13}\text{C}$, $\delta^{18}\text{O}$ and $\delta^2\text{H}$ signatures
703 (in ‰) of the plant-soil compartments (three replicates \pm one standard deviation)
704 measured before and after 1, 2, 8 and 14 days of continuous labelling. A significant
705 enrichment ($\delta^{13}\text{C}$) and depletion ($\delta^{18}\text{O}$, $\delta^2\text{H}$) compared to the unlabelled control (t =
706 0) is highlighted with * (t-test, P < 0.05). The degree of labelling is indicated by the
707 change in the isotopic signature of the last sampling date (t = 14) compared to the
708 control

Sampling date (days)						
$\delta^{13}\text{C}$ (‰)	0	1	2	8	14	14 - 0 ⁽¹⁾
Leaves	-30.8 (± 0.4)	161.5* (± 37.4)	189.7 (± 128.7)	570.7* (± 81.0)	812.5* (± 235.0)	843.3 ± 235.0
Petioles	-32.8 (± 0.2)	163.9* (± 56.2)	212.8* (± 75.2)	908.5* (± 277.3)	941.9* (± 292.7)	974.7 ± 292.7
Stems	-31.4 (± 0.6)	209.6* (± 84.2)	281.3* (± 87.6)	1093.7* (± 402.2)	1119.9* (± 367.6)	1151.3 ± 367.6
Cuttings	-31.2 (± 0.3)	-27.0* (± 1.6)	-26.9 (± 1.9)	-14.6 (± 15.8)	-14.5* (± 2.1)	16.8 ± 2.1
Roots	-30.8 (± 0.7)	98.1* (± 12.5)	90.8 (± 62.9)	646.5 (± 335.1)	618.0* (± 310.9)	648.8 ± 310.9
Bulk soil	-28.0 (± 0.1)	-27.9 (± 0.0)	-27.8 (± 0.2)	-27.5 (± 0.5)	-27.5 (± 0.2)	0.5 ± 0.3
$\delta^{18}\text{O}$ (‰)	0	1	2	8	14	14 - 0 ⁽¹⁾
Leaves	25.9 (± 0.8)	25.2 (± 0.8)	21.9 (± 2.0)	15.0* (± 0.4)	9.0* (± 3.0)	-16.9 ± 3.2
Petioles	21.0 (± 0.2)	20.4 (± 0.4)	19.5* (± 0.4)	14.3* (± 1.6)	12.8* (± 2.3)	-8.2 ± 2.3
Stems	22.4 (± 0.4)	22.2 (± 0.1)	20.6* (± 0.8)	14.7* (± 2.4)	13.3* (± 2.8)	-9.1 ± 2.8
Cuttings	21.3 (± 1.5)	21.9 (± 0.1)	21.8 (± 0.4)	21.5 (± 0.3)	21.5 (± 0.4)	0.2 ± 1.5
Roots	21.2 (± 0.6)	20.6 (± 0.6)	20.9 (± 0.4)	18.2 (± 1.5)	17.5* (± 1.7)	-3.7 ± 1.8
Bulk soil	14.8 (± 0.4)	14.0 (± 0.3)	13.8* (± 0.4)	13.0* (± 0.1)	13.5 (± 0.8)	-1.3 ± 0.9
$\delta^2\text{H}$ (‰)	0	1	2	8	14	14 - 0 ⁽¹⁾
Leaves	-146.6 (± 2.5)		-158.1 (± 7.8)	-169.2* (± 5.5)	-178.0* (± 9.4)	-31.3 ± 9.7
Petioles	-138.3 (± 1.8)				-150.9 (± 6.7)	-12.6 ± 7.3
Stems	-129.2 (± 4.2)		-136.3 (± 4.7)	-153.3 (± 14.8)	-152.9* (± 9.4)	-23.7 ± 10.3
Cuttings	-167.3 (± 2.8)				-172.8 (± 6.3)	-5.5 ± 6.9
Roots	-129.7 (± 6.4)		-134.0 (± 12.5)	-137.0 (± 6.8)	-135.9 (± 7.7)	-6.2 ± 10.0
Bulk soil	-101.5 (± 1.1)				-101.9 (± 1.3)	0.4 ± 1.7

⁽¹⁾ Isotopic difference for the entire labelling experiment

709 **Table 3.** Atomic and isotopic ratios of the labelled bulk organic matter. C/N, O/C and
 710 H/C atomic ratios and $^{18}\text{O}/^{13}\text{C}$ and $^2\text{H}/^{13}\text{C}$ isotopic ratios (of the excess atom fraction)
 711 measured in different plant compartments after the equilibrium in the atmospheric
 712 labelling was reached. Indicated are average values of two sampling dates (t = 8 and
 713 14) with three plant replicates each (\pm one standard deviation)

Compartment	C/N	O/C	H/C	$^{18}\text{O}/^{13}\text{C}^{(1)}$	$^2\text{H}/^{13}\text{C}^{(1)}$
Leaves	13.7 (± 0.4)	0.70 (± 0.01)	1.72 (± 0.04)	0.43 (± 0.07)	0.41 (± 0.06)
Petioles	35.4 (± 1.3)	0.77 (± 0.01)	1.64 (± 0.01)	0.18 (± 0.03)	0.14 (± 0.03) ⁽²⁾
Stems	32.0 (± 4.0)	0.83 (± 0.01)	1.71 (± 0.02)	0.17 (± 0.03)	0.23 (± 0.06)
Cuttings	115.4 (± 7.2)	0.72 (± 0.01)	1.56 (± 0.02)	n.c. ⁽³⁾	n.c. ⁽³⁾
Roots	29.9 (± 2.0)	0.73 (± 0.02)	1.61 (± 0.02)	0.12 (± 0.03)	0.07 (± 0.11)

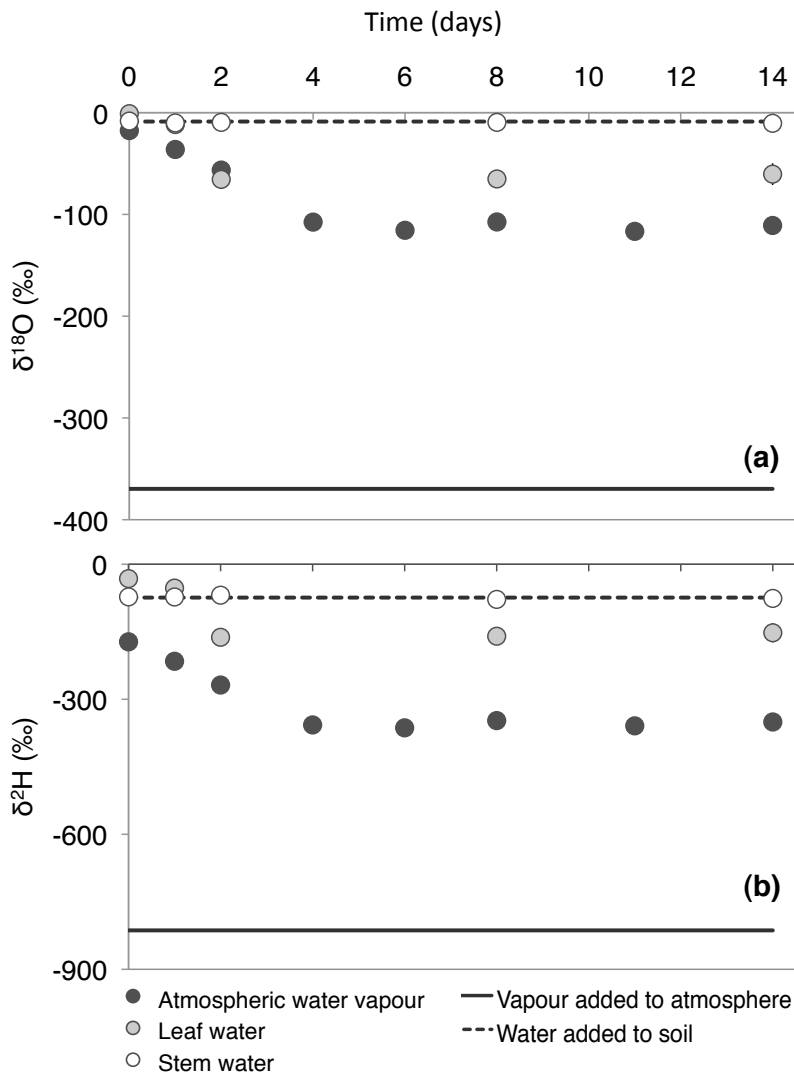
⁽¹⁾ Ratio of excess atom fraction normalized by the maximum label strength (Eq. 7)

⁽²⁾ Only the last sampling date was measured (t = 14)

⁽³⁾ Not calculated (no consistent ^{18}O and ^2H depletion detected in the tissue)

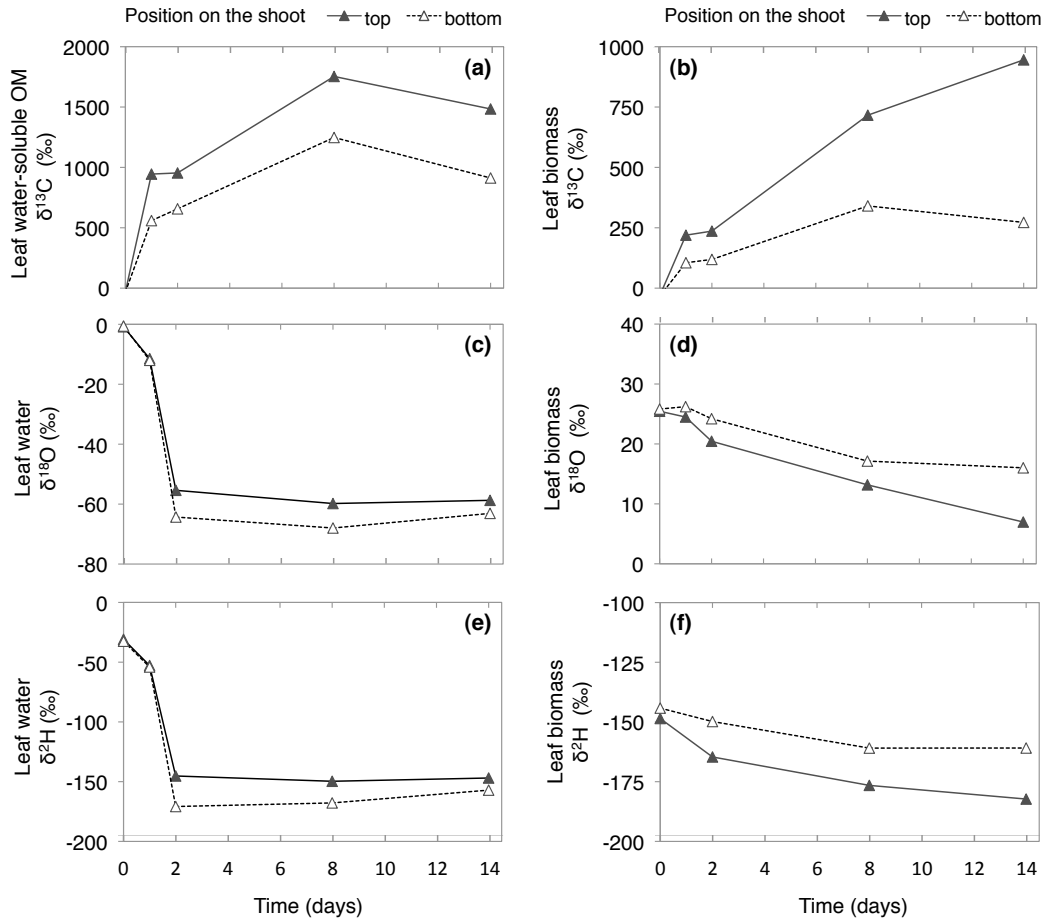
714

714 **Figures**



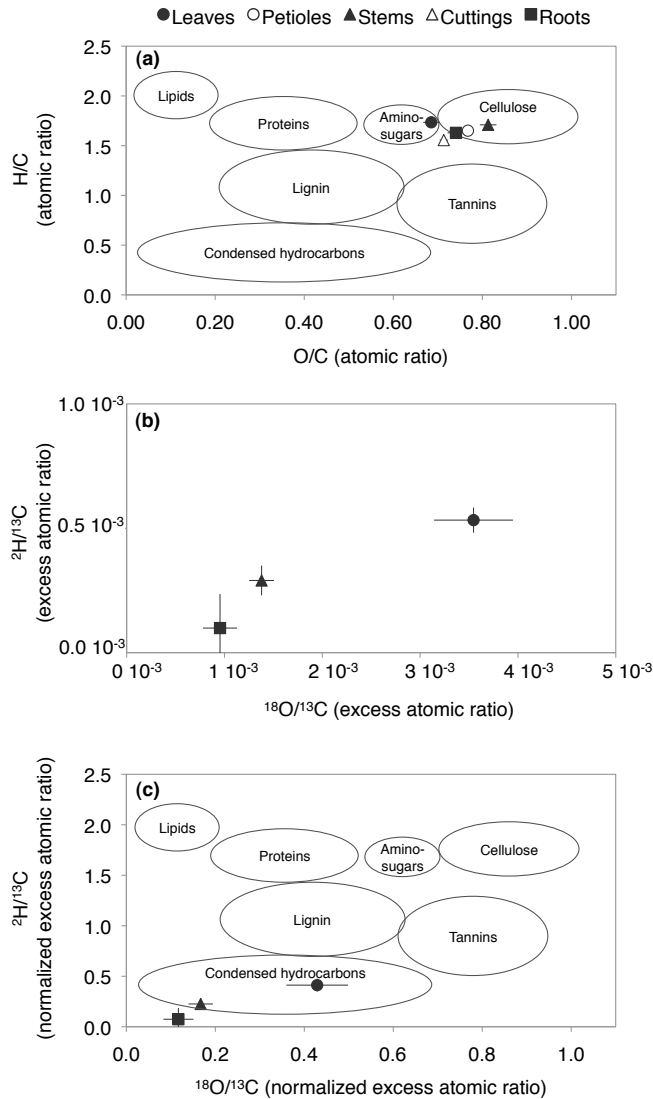
715

716 **Figure 1.** Temporal dynamics in the water isotopic signatures of the plant-soil-
 717 atmosphere system during continuous $^2\text{H}_2^{18}\text{O}$ labelling (a) $\delta^{18}\text{O}$ and (b) $\delta^2\text{H}$ signature
 718 (in ‰) of the depleted water label added as water vapour to the atmosphere (solid
 719 line), of the water added to the soil (dashed line), of the resulting water vapour in the
 720 chamber atmosphere (black dots) and of the extracted leaf (grey dots) and stem water
 721 (white dots). Error bars on the leaf water indicate \pm one standard deviation of three
 722 plant replicates



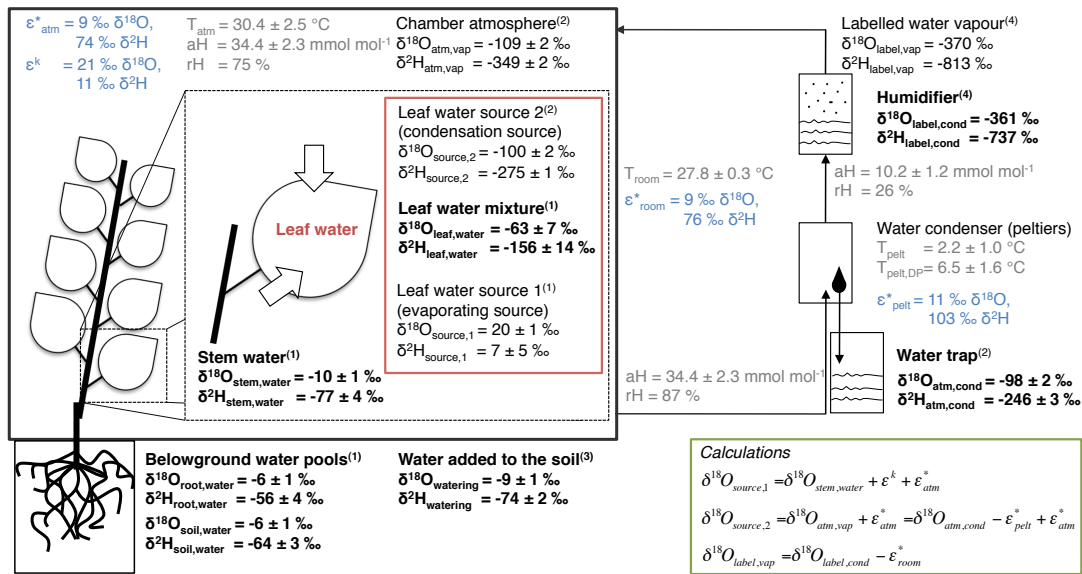
723

724 **Figure 2.** Incorporation of the gaseous labels ($^{13}\text{CO}_2$, $^2\text{H}_2^{18}\text{O}$) into the leaf water
 725 water-soluble and bulk organic matter. (a,b) $\delta^{13}\text{C}$, (c,d) $\delta^{18}\text{O}$ and (e,f) $\delta^2\text{H}$ signature
 726 (in ‰) within leaves sampled at the top (solid line, black triangles), or at the bottom
 727 (dashed line, white triangles) of the shoot. Illustrated are the signatures of (a) the leaf
 728 water-soluble organic matter, (b,e,f) the leaf biomass and (c,e) the leaf water



729

730 **Figure 3.** Atomic and isotopic ratios to illustrate change in organic matter
 731 characteristics (a) Atomic and (b,c) isotopic ratios of oxygen and hydrogen to carbon
 732 within the leaves (closed circles), petioles (open circles), stems (closed triangle), stem
 733 cutting (open triangle) and roots (closed square). The circles overlain on the plots in
 734 (a) and (c) indicate atomic ratios characteristic for different compound classes
 735 (adapted from Sleighter & Hatcher, 2007). (a) illustrates the atomic ratio of all tissues
 736 measured (15 replicates \pm one standard deviation, (b) the isotopic ratios of the ^{13}C ,
 737 ^{18}O and ^2H excess atom fraction (relative to the unlabelled tissues) measured after
 738 equilibrium in the labelling (see Fig. 1 and 2) was reached ($t = 8$ and 14, six replicates
 739 \pm one standard deviation) and (c) shows the isotopic ratios of after normalization with
 740 the maximum label strength of the leaf water (^{18}O , ^2H) and water-soluble organic
 741 matter (^{13}C)



(1) Sampled after 3/12 hours daylight; errors represent variability between plant individuals (three plant replicates each sampling date).
 (2) Integrated value over 2-3 days (water trap analysed at day 6, 8, 11 and 14), errors represent variability between sampling date 8 and 14.
 (3) Average of all watering dates (day 0, 2, 6, 8, 11); errors represent variability between sampling dates.
 (4) Measured at the beginning of the experiment

743
 744 **Figure A1.** Overview on the input data of the two-source isotope mixing model. $\delta^{18}\text{O}$
 745 and $\delta^2\text{H}$ signatures of the water pools of the chamber system are presented as average
 746 values after equilibrium in the labelling was reached ($t = 8$ and 14 days). The
 747 monitored environmental conditions ($T =$ temperature, $a\text{H} =$ absolute humidity and $r\text{H} =$
 748 relative humidity) are presented in grey. The equilibrium and kinetic fractionation
 749 factors, highlighted in blue, were calculated according to Majoube (1971) and Cappa
 750 et al. (2003), respectively. The fractionation factors were used for the calculations
 751 (green box) of the signatures in the non-directly measured pools and the isotopic
 752 signatures of the evaporating and condensation source of the leaf water (red box). The
 753 equations are given for $\delta^{18}\text{O}$, but apply for $\delta^2\text{H}$ analogously. Please note that the data
 754 reported here are average values of the two last sampling dates, while we present in
 755 the result section the data of single sampling dates or average values of the whole
 756 labelling experiment (environmental conditions, equilibrium fractionation factors)

757 **Appendix B**

758 Calculation of the relative air humidity and the dew-point temperature

759 The dew-point temperature, i.e. the temperature at which the water condensed inside
 760 the peltier-cooled water condenser ($T_{\text{pelt,DP}}$) was calculated by solving Equation B1
 761 with the humidity measured in the air after the condenser ($10 \pm 1 \text{ mmol mol}^{-1}$ $a\text{H}$, 26
 762 % $r\text{H}$).

763
$$rH(T) = \frac{e}{e(T)} \cdot 100 \tag{B1}$$

764 , where rH is the relative air humidity (in %), e is the partial pressure of water vapour
765 (calculated according to Eq. B2) and e(T) is the saturation vapour pressure (in kPa,
766 calculated according to Eq. B3).

767
$$e = \frac{aH}{1000} \cdot p \tag{B2}$$

768 , where aH is the absolute humidity given as the mole fraction of water vapour (mmol
769 mol⁻¹) and p is the atmospheric pressure (in kPa).

770
$$e(T) = 0.61365 \cdot e^{\frac{17.502 \cdot T}{240.97 + T}} \tag{B3}$$

771 , where T is the room air temperature (in °C).

772 References

773 Cappa C.D., Hendricks M.B., Depaolo D.J. and Cohen R.C.: Isotopic fractionation of
774 water during evaporation. *J Geophys. Res.*, 108,: 4525. doi: 10.1029/2003
775 JD003597, 2003.

776 Majoube M.: Fractionnement en oxygène 18 et en deutérium entre l'eau et sa vapeur.
777 *J. Chim. Phys. physico-chimie Biol.*, 68,1423–1435. 1971.